PLANNED INVESTIGATION OF INFRARED EMISSIONS ASSOCIATED WITH THE INDUCED SPACECRAFT GLOW: A SHUTTLE INFRARED GLOW EXPERIMENT (SIRGE)

Michael J. Mumma and Donald E. Jennings

Planetary Systems Branch, Laboratory for Extraterrestrial Physics, NASA/Goddard Space Flight Center

Abstract. We will investigate the characteristics of infrared molecular emissions induced by energetic collisions between ambient atmospheric species and surfaces in Earth orbit, using low-resolution infrared spectroscopy. The spectrometer will be a liquid-nitrogen-cooled filter wheel photometer covering the wavelength range 0.9-5.5 microns with a resolving power ($\lambda/\Delta\lambda$) of approximately 100. This resolving power will be sufficient for identification of the molecular or atomic fluorescent species causing the glow.

Introduction

The instrument to be used for the Shuttle Infrared Glow Experiment (SIRGE) will be a liquid nitrogen cooled spectrometer flown in a GAS canister in the Hitchhiker-G program. With it, we will study the infrared (0.9-5.5 micron) component of the induced shuttle glow [Abreu et al., 1983; Banks et al., 1983; Langhoff et al., 1983; Mende et al., 1983; Slanger, 1983; Yee and Abreu, 1983]. The spectrometer uses a circular variable filter (CVF) to provide a spectral resolving power ($\lambda/\Delta\lambda$) of 100 and a sensitivity (single scan NESR) of less than 2×10^{-14} watts/cm^2 sr cm^{-1}. This is necessary to reach the zodiacal light limit, which is considered the limiting flux source for astronomy in the near infrared. The infrared glow study has been requested by the Hubble Space Telescope (HST) project office because of concern expressed by the astronomical community regarding the impact which a glow from HST might have on the feasibility of infrared observations, and on the choice and design of infrared instruments for HST. It has also been proposed (C. R. O'Dell, private communication) that the infrared glow spectrometer be flown on the HST deployment mission, to determine the magnitude and character of the glow surrounding the telescope after ejection from the shuttle. The glow near the shuttle itself will be studied on this and subsequent missions to help characterize and model the emission so that predictions can be made for various spacecraft and various altitudes. The high sensitivity and moderate resolution specified for this instrument are necessary for a complete characterization of the glow.

Instrument Specifications

Figure 1 shows a conceptual drawing of the SIRGE instrument. Table 1 lists the basic specifications. The spectrometer will be mounted in a liquid nitrogen dewar, and housed in a Getaway Special (GAS) can. The instrument will be mated with the Hitchhiker-G avionics, and mounted on a single GAS beam for ease of manifesting on the space shuttle (Figure 2).

The inner liquid nitrogen container will be supported within the GAS can with a thermally isolated structure, and will be radiatively shielded with multiple-layer-insulation. Fill and vent ports will be provided, along with a pumping port for the dewar vacuum jacket, and these will be accessible from the top of the GAS can. The effluent gas will be routed away from the vicinity of the optical aperture to avoid potential modification of the local glow effects on orbit. A sealed aperture door will open in orbit to expose the instrument to the glow. This door will also provide a radiation (heat) shield for the aperture during the ground hold time. A sun sensor will close the door automatically. The dewar will have a minimum hold time of 15 days, including 5 days pre-launch hold time. The dewar will be filled with a carbonized rayon porous material to prevent phase separation in zero gravity. The dewar will be vented through a pressure regulator, maintaining the temperature of the liquid nitrogen at 65 kelvin (or lower, TBD).

The spectrometer will use entirely reflective optics (except for the CVF) to reduce scattered light and improve throughput (Figure 3). Reflective optics provide several additional advantages, principally related to the absence of dispersion. Thus, all wavelengths are focussed simultaneously at the same point, and the wavelength response can be extended in future by replacing only the detectors and the wavelength-selecting filters. Alignment can be carried out at visual wavelengths, and the parabolic mirrors can be diamond-machined under numerical control, which greatly assists assembly and alignment.

The input aperture will be baffled to minimize scattered light, e.g. from the Sun, Earth, and Moon. Rejection of off-axis stray light will be further enhanced with a Lyot stop in the fore-optics (Figure 3). The field-of-view of the spectrometer will be 4° x 4° square and the collecting aperture will be 0.6 inch diameter. After passing the Lyot stop, the collected radiation is re-focussed onto a circular-variable-filter wheel (CVF) where wavelength selection occurs. The CVF will have three sections, variable in wavelength: 0.9-1.8, 1.5-3.0, and 2.7-5.5 microns. The spectral resolution of the CVF is 1% of the wavelength. All filter components are available commercially. The transmitted radiation is re-focussed onto an infrared detector (InSb), operated at 65 kelvin (or lower) to provide an NESR of less than 2×10^{-14} watts/cm^2 sr cm^{-1} in a 5-second scan. The scan time will be as short as is possible ($\sim$5 seconds) without degrading sensitivity due to bandwidth limitations. The detector will use a trans-impedance amplifier with a load resistor of approximately 2×10^{10} ohms. A stimulator (infrared source) will be located in the pre-optics area to provide an internal calibration source. The expected instrument sensitivity is compared with the zodiacal background, with various external calibration objects, and with possible glow intensities in Figure 4.

A second detector will be provided in the pre-optics area to be used in the broadband mode. It will be sampled at the same rate as the narrow-band detector in the focal plane, but will observe the full spectrum at once to monitor rapid changes in the glow flux level (during thruster firing, for instance) and to measure very weak fluxes. The flight electronics will oversample the focal plane detector signal by a

factor of 5-10 and provide a dynamic range of 10^5. Additional channels will be provided for the broadband detector and several temperature sensors. The output of the electronics will be compatible with the Hitchhiker avionics. The power and instrument control lines, and the data lines, will be routed through the bottom of the GAS can (Figure 1). The power and instrument control will be supplied via the Hitchhiker avionics. Data will be recorded onboard and also downlinked to ground support equipment, providing direct control of the experiment and real-time data inspection during flight.

The entire assembly will be compatible with GAS/shuttle launch and orbit conditions, and will satisfy structural, thermal, and safety requirements for GAS payloads. The entire flight instrument will be contained in a single GAS can, so that the Hitchhiker avionics and instrument GAS canister can be flown on a single GAS beam (Figure 2).

Sensitivity

InSb detectors near 1 mm in diameter and having high sensitivity are commercially available, and will be used. The optical throughput (etendue) is then easily calculated from the f/.83 detector focussing mirror to be

$$A\Omega = 1.03 \times 10^{-2} \text{ cm}^2 \text{ sr} \tag{1}$$

This etendue is preserved throughout the optical system. The collecting mirror at the entrance aperture has an effective diameter of 3.14 cm and is operated at f/1.6. The field stop is 4 mm x 4 mm, corresponding to a square beam on the sky of 4.5° x 4.5°.

The Noise-Equivalent-Spectral-Radiance (NESR), for an extended source of uniform surface brightness which fills the field-of-view, is given by

$$NESR = \frac{NEP}{TA\Omega \ \Delta\nu \ \sqrt{\tau}} \quad \text{watts/cm}^2 \text{ sr cm}^{-1} \tag{2}$$

where

NEP	$= (10^{-4} \ \nu)NEP1$, the detector NEP at frequency ν (cm^{-1}),
NEP1	$= 1.8 \times 10^{-15}$ W/$\sqrt{Hz}$, the NEP at $\lambda = 1 \mu m$ wavelength,
T	$= 0.4$, the total transmittance of the optical system,
AΩ	$= 1.03 \times 10^{-2}$ cm^2 sr, the etendue,
$\Delta\nu$	$= \nu/R$, the spectral resolution element,
R	$= 100$, the spectral resolving power,
t	$= \tau_i/R$, the integration time per spectral element,
τ_i	$= 5$ seconds, the integration time required for one complete scan,
N	$=$ the number of complete scans, and
τ	$= N\tau_i$, the total integration time.

252

Then,

$$NESR = \frac{10^{-4} \ R^{3/2} \ NEP1}{TA\Omega \ \sqrt{\tau}} \ watts/cm^2 \ sr \ cm^{-1} \qquad (3)$$

or, using the values given above,

$$NESR = \frac{4.36 \times 10^{-14}}{\sqrt{\tau}} \ watts/cm^2 \ sr \ cm^{-1} \qquad (4)$$

Note that the NESR expressed in equations (3) and (4) is independent of wavelength, if the resolving power is kept constant.

It is also useful to express the NESR in units of Rayleighs/$\overset{o}{A}$ (the Rayleigh is a unit of surface brightness equivalent to 10^6 photons $cm^{-2} \ sec^{-1}$, radiated into 4π sr),

$$NESR = \frac{4\pi \cdot 10^{-18} \ \nu_c \ R^{3/2}}{hc \ TA\Omega \ \sqrt{\tau}} \ Rayleighs/\overset{o}{A} \qquad (5)$$

For the parameters given above, the NESR may be re-written

$$NESR = \frac{2.75}{\lambda \ \sqrt{\tau}} \ Rayleighs/\overset{o}{A} \qquad (6)$$

where λ is given in μm. The expected NESR is shown in Figure 4 for $\tau=100$ seconds and a resolving power of 100, representing $\sim$20 co-added spectral scans.

For faint continuum emissions, the spectral resolving power can be degraded in software by $\sim$10-fold (to R = 10), providing an NESR of 1.4 x 10^{-16} W/$\sqrt{Hz}$ for $_\tau$ = 100 seconds. This is compared with the intensity of the zodiacal light towards the ecliptic pole in Figure 4, where it is seen that good signal-to-noise can be obtained on this important astronomical background source. The zodiacal light is typically 2-3 times brighter in the ecliptic plane, at 90° elongation. The apparent mean surface brightness of Mars, Jupiter, and Saturn, diluted to our beam size in August 1986, are also shown. Spectral structure has been omitted for representation purposes.

The strongest emissions of all may be those of the induced glow. For example, if the unresolved continuum level seen in the ISO spectra ($\sim$50 R/$\overset{o}{A}$ at 0.6 μm, Torr and Torr [1984]) were assumed to be due to OH Meinel band emission, then Langhoff's spectral model could be used to estimate the intensity expected at 1.5 μm [Langhoff et al.,1983]. According to this model, it would be $\sim$30 times brighter there. The ratio of signal-to-noise expected using the SIRCE spectrometer (single scan, τ = 5 seconds) would then be $\sim$1800. However, this is probably an over-estimate for the OH intensity. In addition to potential OH emission, other bands may be present such as NO_2 ($\nu_1 + \nu_3$, and ν_3), H_2O (ν_1 and ν_3), NO (1-0, overtones, and hot bands), N_2O (ν_3), CO (fundamental, overtones, hot bands), and CO_2 (ν_3), to mention only those which have been suggested or which seem particularly likely.

The flux seen by the detector must be $< 2.5 \times 10^{-12}$ watts, for the NEP used, if amplifier saturation is to be avoided. Hence, the beam averaged surface brightness (at 1 μm) cannot exceed

$$R_{max} = 2.5 \times 10^{-12} \text{ watts/cm}^2 \text{ sr cm}^{-1} \tag{7}$$

Thus, the maximum signal-to-noise ratio achievable in a single scan will be ∿125. If the induced glow were to be as bright as indicated in Figure 4, our amplifiers would be saturated, therefore a commandable ranging capability is included in the electronics design.

Test and Calibration

Careful optical calibration and testing will be conducted in the laboratory, with particular emphasis on measurements of the off-axis rejection of stray light, the absolute intensity calibration, the noise performance, and the measurement of linearity. Additional tests (vibration, thermal, EMI) will be carried out, as required.

Particular emphasis will be placed on intensity calibration. Ground calibration of the assembled system will be carried out in the laboratory, before and after flight. However, because of the long time (probably 1 year) between the calibrations, we plan to make in-flight calibration as well. An internal infrared source (stimulator, Figure 3) will provide relative intensity calibration, and external sources (Mars, Jupiter, Saturn, Figure 4) will provide absolute calibration. The external sources can be acquired by pointing the space shuttle, since our large beam size permits source acquisition with only modest pointing accuracy. Terrestrial limb scans will enable intensity, wavelength, and dynamic range calibration from the known OH Meinel airglow itself. Finally, when viewing deep space, the zodical emission provides an automatic signal for calibration of faint glow emissions.

References

Abreu, V. J., W. R. Skinner, P. B. Hays, and J. H. Yee, Optical effects of spacecraft-environment interaction: Spectrometric observations by the DE-B satellite, AIAA-83-2657-CP, presented at Shuttle Environment and Operations Meeting, Washington, D.C., 1983.

Banks, P. M., P. R. Williamson, and W. J. Raitt, Space Shuttle glow observations, Geophys. Res. Lett., 10, 118-121, 1983.

Langhoff, S. R., R. L. Jaffe, J. H. Yee, and A. Dalgarno, The surface glow of the Atmospheric Explorer C and E satellites, Geophys. Res. Lett., 10, 896-899, 1983.

Mende, S. B., O. K. Garriott, and P. M. Banks, Observations of optical emissions on STS-4, Geophys. Res. Lett., 10, 122-125, 1983.

Slanger, T. G., Conjectures on the origin of the surface glow of space vehicles, Geophys. Res. Lett., 10, 130-132, 1983.

Torr, M. R., and D. Torr, Preliminary results of the imaging spectrometric observatory on Spacelab 1, AIAA-84-0044, presented at AIAA 22nd Aerospace Sciences Meeting, Reno, 1984.

Yee, J. H., and V. J. Abreu, Visible glow induced by spacecraft-environment interaction, Geophys. Res. Lett., 10, 126-129, 1983.

TABLE 1. SHUTTLE INFRARED GLOW EXPERIMENT: SPECIFICATIONS AND REQUIREMENTS

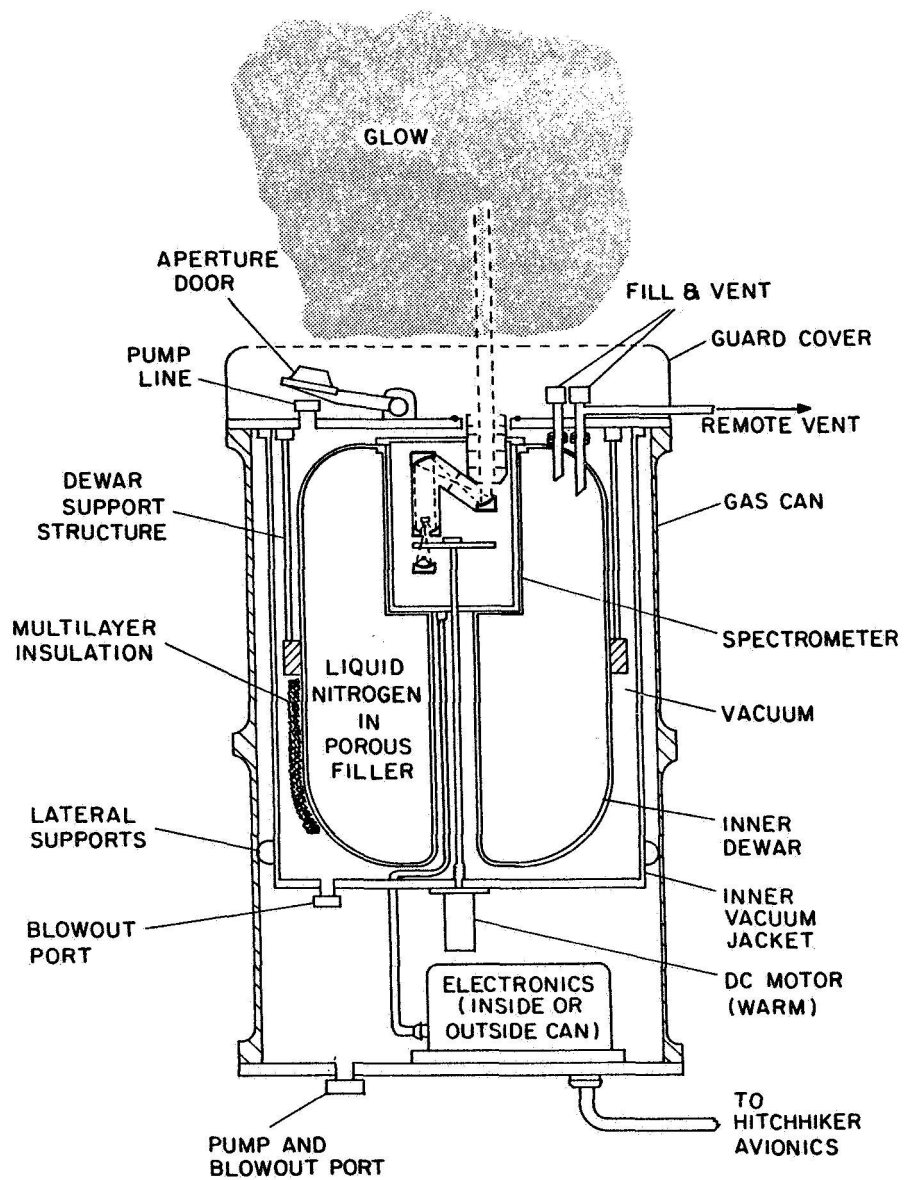|	
Wavelength Coverage	0.9-5.5 microns
Resolving Power	100
Detector	InSb
Sensitivity (single scan NESR)	$<2 \times 10^{-14}$ W/cm^2 sr cm^{-1}
Scan Time	$\lesssim 5$ seconds
Operating Temperature	<65 K
Dewar Hold Time (minimum)	5 days pre-flight 10 days in-flight
Field-of-View	$4^{\circ} \times 4^{\circ}$
Aperture Size	3.14 cm diameter

Fig. 1. Conceptual drawing of SIRGE instrument in GAS can.

LOOK DIRECTION

OPENING LID

ORBITER SILL

VENT LINE

FILL PORT

VACUUM PUMPING
PORT

GAS CAN
WITH SIRGE

GAS BEAM
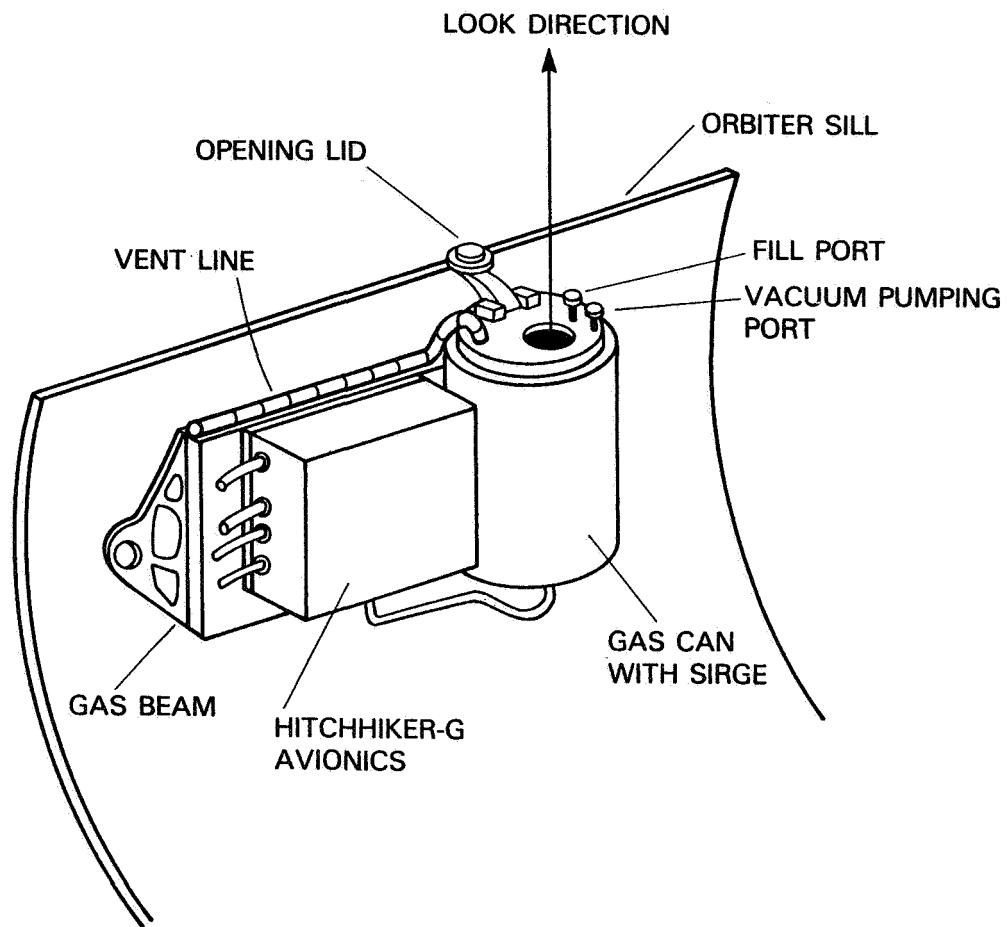
HITCHHIKER-G
AVIONICS

Fig. 2. SIRGE spectrometer Hitchhiker mounting configuration.
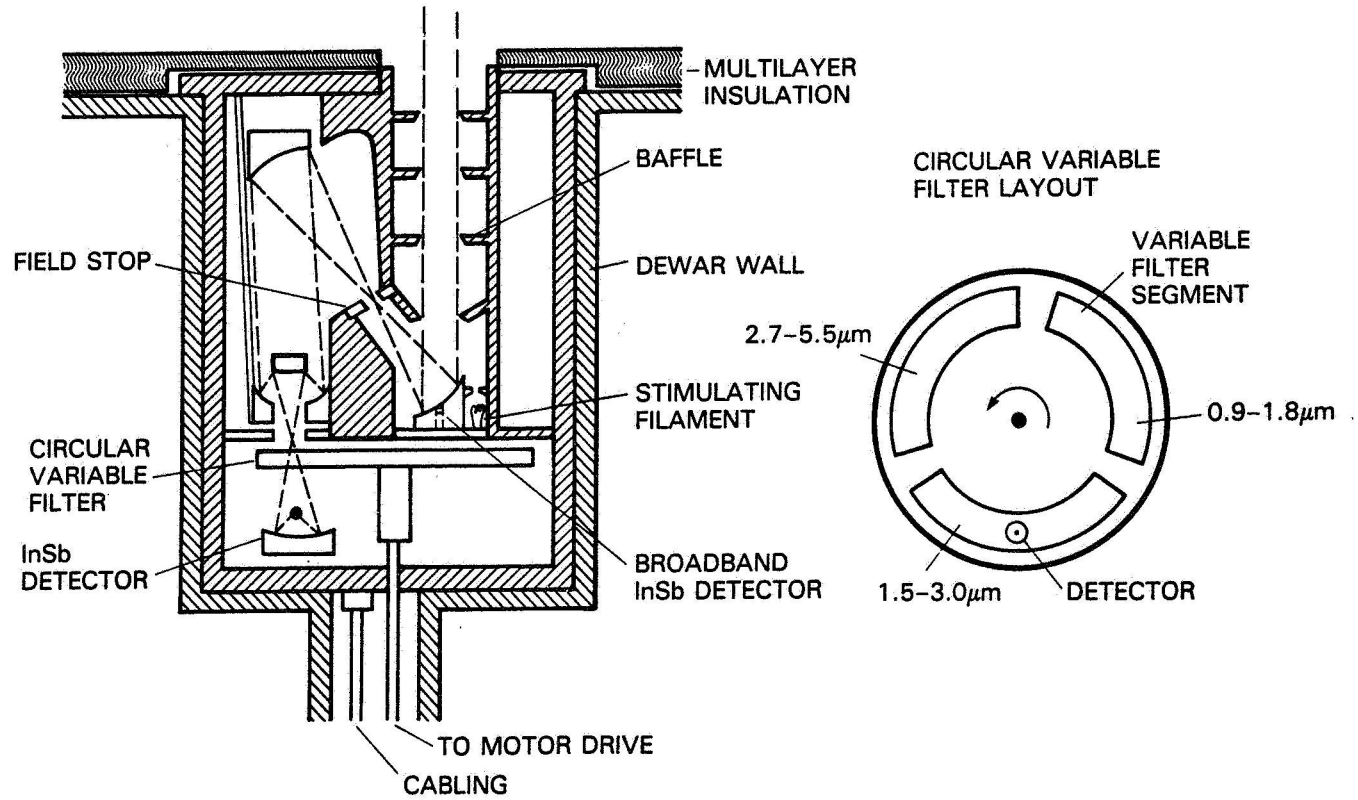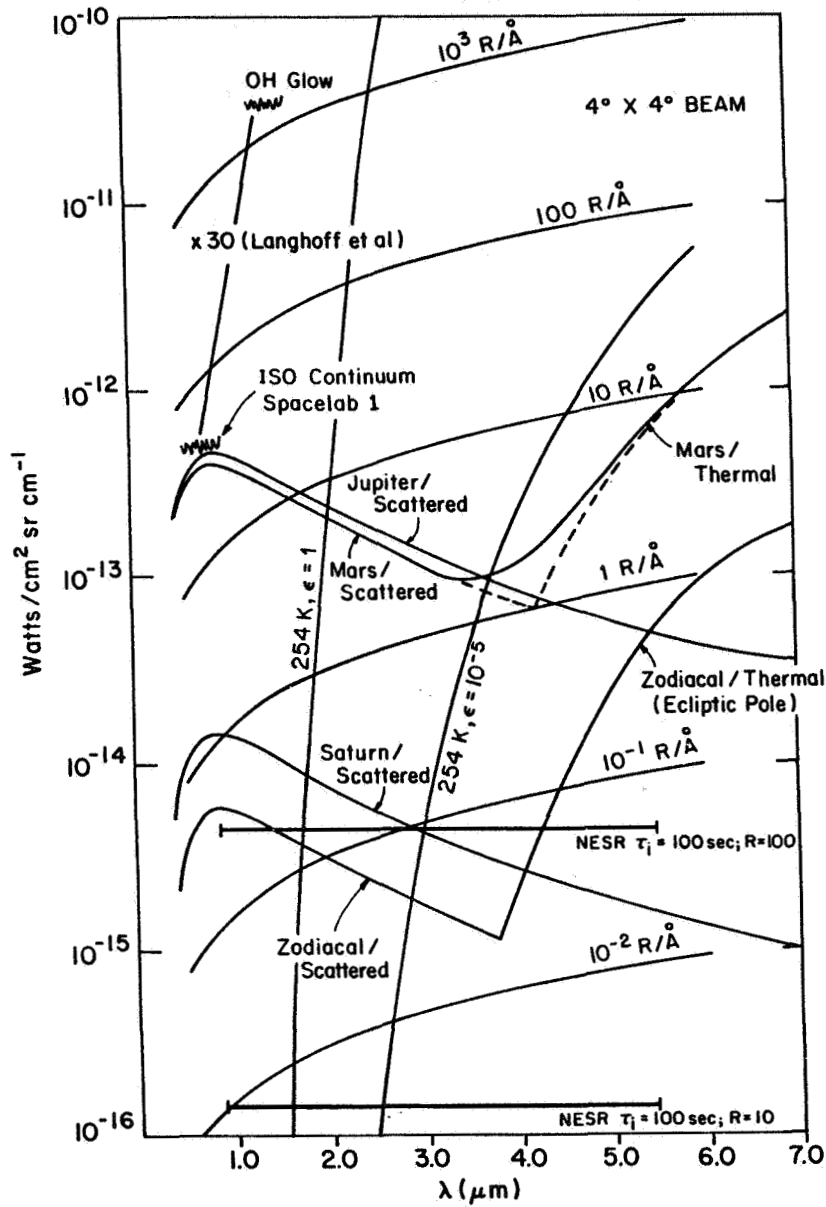
Fig. 3. SIRGE spectrometer optical layout.

Fig. 4. SIRGE sensitivity limits, calibration sources, and possible glow intensities.